JOURNAL OF THERMOPHYSICS AND HEAT TRANSFER
Vol. 12, No. 4, October–December 1998

# Transport Properties of Hydrogen

James R. Stallcop*
*NASA Ames Research Center, Moffett Field, California 94035-1000*
Eugene Levin†
*Eloret Corporation, Moffett Field, California 94035-1000*
and
Harry Partridge‡
*NASA Ames Research Center, Moffett Field, California 94035-1000*

**Transport cross sections and collision integrals have been calculated for interactions of hydrogen atoms and diatomic molecules. These results were determined using accurate potential energies and quantum mechanical formulations of the scattering. Collision integrals have been tabulated for H–H and $H_2$–$H_2$, and have been applied to determine diffusion and viscosity. The variation of transport properties with temperature and relative composition is examined for a gas formed from H atoms and $H_2$ molecules. The inversion temperature is found to be about a factor 3 lower than that of earlier estimates.**

## Nomenclature

$a_0$ = Bohr radius, $5.291772 \times 10^{-9}$ cm
$D$ = coefficient of diffusion, $cm^2/s$
$D^*$ = reduced coefficient of diffusion
$E$ = collision energy, $E_h$
$k$ = wave number
$l$ = angular momentum quantum number
$P$ = Legendre polynomial
$p$ = pressure, atm
$Q$ = transport cross section, $a_0^2$
$r$ = separation distance, $a_0$
$T$ = temperature, K
$V$ = potential energy, $E_h$
$\alpha$ = thermal diffusion factor
$\gamma$ = polar angle
$\eta$ = coefficient of viscosity, g/(cms)
$\eta^*$ = reduced coefficient of viscosity
$\kappa$ = Boltzmann constant
$\mu$ = reduced mass, amu
$\sigma^2\Omega$ = collision integral, $Å^2$
$\phi$ = azimuthal angle

## Introduction

THE transport properties of hydrogen are needed for studies of heavy-planet atmospheric entry and certain propulsion systems for satellites and other space vehicles.[1] Transport data for hydrogen have been calculated by Vanderslice et al.[2] from approximate potential energies. Some of these results have been improved by Svehla,[3] using approximate theoretical results and experimental data. Accurate potential energies have been calculated for the interaction of the atoms and ions of air and a number of interactions involving molecules; we have applied these results to the determination of transport data.[4,5] Our tabulations of calculated transport data are extended to include the interactions for the atoms and molecules of hydrogen in the present work. We have applied the best interaction data in a quantum mechanical calculation of the scattering to obtain accurate transport data. Thus, the present results at low energies or temperatures are preferable to the corresponding results that were obtained using classical mechanics.[3] The H–H results are expected to be accurate to three or four significant figures. The present tabulations for $H_2$–$H_2$ allow a more definitive determination of transport properties above the highest temperature (about 600 K) of the absolute measurements of the viscosity. The transport properties of a mixture can be determined to second-order using the results of our tabulations. The results of this work are also important for developing combining relations to determine transport properties for the collisions of complex molecules.[6]

## Interaction Potential Energies

Accurate H–H interaction energies have been calculated by Kołos and Wolniewicz.[7,8] We have extended these results to large separation distances $r$ using extremely well-known values of the dispersion coefficients.[9,10] The potential energy surface for H–$H_2$ interactions has been calculated accurately by Partridge et al.[11]; the position $r_m$ of the well minimum and the well depth $\bar{V}_m$ of the spherically averaged potential energy $\bar{V}(r)$ are predicted to be $6.51 \pm 0.03a_0$ and $75 \pm 3\ \mu E_h$, respectively. The potential energies are extended to large $r$ with the dispersion coefficients calculated by Bishop and Pipin[12] and by Meyer, which are found in Ref. 13. We have shown that the theoretical $\bar{V}(r)$ agrees well with the corresponding result deduced from scattering measurements.[14] Schaefer and Köhler[15] determined a potential energy surface for $H_2$–$H_2$ interactions by an adjustment of ab initio potential energies to yield calculated data that agree with measured values of the second virial coefficient and measured scattering cross sections; the values of $r_m$ and $\bar{V}_m$ are $6.50a_0$ and $111.7\mu E_h$, respectively. Their interaction energies have been shown to reproduce discriminating spectroscopic measurements.[16–18]

The repulsive wall of the $H_2$–$H_2$ potential energy surface is not very sensitive to the measurements.[15] Furthermore, the potentials deduced from scattering measurements are not necessarily unique.[14] Only the leading term $\bar{V}(r)$ in an expansion of the ab initio energies in spherical harmonics requires adjustment to provide a fit to measured virial data, primarily, because the potential anisotropy is found to be small.[15] Consequently, the small uncertainty in the repulsive wall of Ref. 15 for small $r$ can be readily reduced by the application of more accurate values of $\bar{V}(r)$.

Received Feb. 18, 1998; revision received June 30, 1998; accepted for publication July 1, 1998. 

*Physicist, Computational Chemistry Branch, Space Technology Division, M/S 230-3.
†Senior Research Scientist, Thermosciences Institute, M/S 230-3.
‡Chemist, Computational Chemistry Branch, Space Technology Division, M/S 230-3.

A careful calculation of the interaction energy (that are free of the basis set superposition error[19]) tends to overestimate the repulsive energy because of the difficulty in obtaining convergence even for the simplest molecular systems. We have found that a rotation of the short-range repulsion energy $V_{SR}$ is suitable for lowering ab initio potential energies to fit measured virial data.[19] This procedure retains the interaction energy at large $r$, which is necessary when the long-range force constants are known accurately, and also accounts for the decreasing relative error in ab initio calculations at small $r$. The repulsive potential at small $r$ for the present calculations has been obtained from the $V_{SR}(r)$ that is determined from the ab initio $\bar{V}(r)$ of Meyer et al.[20] that have been rotated at the crossing point $r_x = 3.5a_0$ to fit $\bar{V}(5a_0)$ listed in Ref. 15. This lowering of the ab initio potential energy was selected to accomodate a fit at the highest temperature (423 K) of the measurements of the second virial coefficient of para hydrogen.[21] This potential modification results in a slight lowering (by at most about 1%) of the viscosity coefficient relative to the corresponding values[14] obtained from the potential energy of Ref. 15 at high temperatures.

## Calculation of Transport Cross Sections and Collision Integrals

Assuming electron-spin degeneracy, for H–H interactions we have taken the mean transport cross section $\bar{Q}_n(E)$ for a collision energy $E$ to be the degeneracy-weighted average[22]

$$\bar{Q}_n(E) = \tfrac{1}{4}Q_n^X(E) + \tfrac{3}{4}Q_n^b(E) \tag{1}$$

where $Q_n^X(E)$ and $Q_n^b(E)$ are the cross sections for the bound $X^1\Sigma_g^+$ and the primarily repulsive $b^3\Sigma_u^+$ states, respectively.

When one or both of the collision partners is a molecule, we apply the formulation of Parker and Pack[23] that was derived using centrifugal and sudden approximations. Thus, for H–$H_2$ collisions, $\bar{Q}_n(E)$ has been obtained from an average over orientations

$$\bar{Q}_n(E) = \int_0^{\pi/2} d\gamma Q_n(E, \gamma)\sin\gamma \tag{2}$$

where the polar angle $\gamma$ describes the geometry of the colliding pair as described in Ref. 24. A transformation has been applied to convert the $H_2$–$H_2$ potential energy surface of Ref. 15 from the space-fixed frame to the body-fixed frame; the appropriate average $\bar{Q}_n(E)$ was then calculated from

$$\bar{Q}_n(E) = \frac{1}{\pi}\int_0^{\pi} d\phi \int_0^{\pi/2} d\gamma_1 \int_0^{\pi/2} d\gamma_2 \times Q_n(E, \gamma_1, \gamma_2, \phi)\sin\gamma_1 \sin\gamma_2 \tag{3}$$

where $\gamma_i$ is the polar angle for the $i$th molecule, and the azimuthal angle $\phi$ specifies the relative orientation of the two molecules.

Consistent with a quantum mechanical formulation of the scattering,[23] the transport cross sections $Q_n$ are determined from the scattering phase shifts $\eta_l$ that are calculated from the central-field potential energy for a state of Eq. (1) or an orientation specified by the angles of Eqs. (2) and (3), i.e.,

$$Q_n = \frac{4\pi}{k^2}\sum_{l=0}^{\infty}\sum_{v>0}^{n} a_{nv}^l \sin^2(\eta_{l+v} - \eta_l) \tag{4}$$

where the allowed values of $v$ are even or odd according to the parity of $n$. The coefficients $a_{nv}^l$ can be determined from recursion relations.[25]

The mean collision integrals $\sigma^2\bar{\Omega}_{n,s}(T)$ are determined from an average over a Maxwell-Boltzmann velocity distribution,[20] i.e.,

$$\sigma^2\bar{\Omega}_{n,s}(T) = \frac{F(n, s)}{2(\kappa T)^{s+2}}\int_0^{\infty} e^{-E/\kappa T}E^{s+1}\bar{Q}_n(E)\, dE \tag{5}$$

where $\kappa$ is the Boltzmann constant, $T$ is the kinetic temperature, and $F(n, s)$ is a hard-sphere factor.[23]

The $\eta_l(E)$ have been calculated at lower $E$ from a numerical integration of the Schroedinger equation, using the method presented by Levin et al.[26] A semiclassical method is used to determine $\eta_l(E)$ at $E$ above a threshold energy $E_t$, where the difference in the cross sections between the two methods does not exceed 0.3%.[25] (Hence, there is a small uncertainty in the cross sections of the present calculation for a small range of $E$ above $E_t$.)

The numerical integrations of Eqs. (2) and (3) have been carefully performed to assure that interpolated values of $Q_n$ for orientations near the endpoints of the integral reflect the symmetry of the collision pair and that the orientations selected are sufficient to provide convergence.

We have shown that the sudden approximations yield H–$H_2$ collision integrals that are accurate[14]; i.e., our calculated values of the diffusion and viscosity coefficients agree with the cor-

**Table 1 H–H mean transport cross sections ($a_0^2$)**

| $E(E_h)$ | $\bar{Q}_1(E)$ | $\bar{Q}_2(E)$ | $\bar{Q}_3(E)$ |
|---|---|---|---|
| 0.0060 | 72.08 | 54.77 | 82.79 |
| 0.0080 | 71.89 | 55.78 | 81.70 |
| 0.0100 | 66.33 | 50.95 | 75.26 |
| 0.0120 | 61.38 | 47.46 | 71.51 |
| 0.0150 | 57.83 | 44.80 | 66.81 |
| 0.0200 | 52.34 | 40.29 | 61.33 |
| 0.0300 | 44.25 | 34.79 | 52.55 |
| 0.0400 | 40.34 | 32.33 | 48.56 |
| 0.0500 | 38.70 | 29.42 | 46.05 |
| 0.0600 | 35.20 | 27.61 | 42.47 |
| 0.0800 | 27.58 | 26.98 | 34.57 |
| 0.1000 | 22.11 | 24.75 | 30.45 |
| 0.1500 | 14.50 | 18.40 | 23.45 |
| 0.2000 | 10.66 | 14.11 | 18.43 |
| 0.3000 | 6.80 | 9.36 | 12.46 |
| 0.4000 | 4.88 | 6.85 | 9.20 |
| 0.5000 | 3.74 | 5.33 | 7.19 |
| 0.6000 | 3.00 | 4.32 | 5.85 |

**Table 2 H–$H_2$ mean transport cross sections ($a_0^2$)**

| $E(E_h)$ | $\bar{Q}_1(E)$ | $\bar{Q}_2(E)$ | $\bar{Q}_3(E)$ |
|---|---|---|---|
| 0.0001 | 121.86 | 101.73 | 143.08 |
| 0.0002 | 102.42 | 83.09 | 117.81 |
| 0.0003 | 94.15 | 75.06 | 107.45 |
| 0.0005 | 85.11 | 68.91 | 96.86 |
| 0.0007 | 79.54 | 64.91 | 90.77 |
| 0.0010 | 73.80 | 60.92 | 84.71 |
| 0.0020 | 62.89 | 53.44 | 73.49 |
| 0.0030 | 56.60 | 49.10 | 67.07 |
| 0.0040 | 52.16 | 46.00 | 62.53 |
| 0.0050 | 48.73 | 43.59 | 59.01 |
| 0.0060 | 45.95 | 41.62 | 56.14 |
| 0.0080 | 41.58 | 38.48 | 51.62 |
| 0.0100 | 38.22 | 36.04 | 48.12 |
| 0.0150 | 32.21 | 31.58 | 41.79 |
| 0.0200 | 27.97 | 28.39 | 37.33 |
| 0.0300 | 22.39 | 23.75 | 31.16 |
| 0.0400 | 18.81 | 20.50 | 26.94 |
| 0.0500 | 16.31 | 18.10 | 23.83 |
| 0.0600 | 14.46 | 16.24 | 21.42 |
| 0.0800 | 11.86 | 13.54 | 17.92 |
| 0.1000 | 10.12 | 11.68 | 15.48 |

responding results from close-coupling calculations to within 1%. The theoretical diffusion agrees well with measurements at room temperature.[14] Furthermore, we have also shown that our calculated viscosity for $H_2$–$H_2$ collisions agrees well with the corresponding measured results in the low-$T$ region, where the uncertainty in the experimental data is relatively small.[14]

The cross sections are needed to determine the transport properties when a Maxwellian velocity distribution is not applicable. The cross sections $\bar{Q}_n(E)$ for H–H collisions exhibit an oscillatory behavior in the low-$E$ region[26] (primarily, the structure of the cross sections arises from resonance scattering[27] because of the relatively deep potential well of the ground state); the values at high $E$ are slowly varying and are shown in Table 1. The cross sections for H–$H_2$ collisions are listed in Table 2. The values of $\sigma^2\bar{\Omega}_{n,s}(T)$ that were obtained using Eq. (5) for H–H interactions are contained in Table 3; the results for H–$H_2$ interactions can be found in Table 2 of Ref. 14. The large set of $\bar{Q}_n(E)$ for H–H interactions that are required to obtain the convergence shown in Table 3 are available from the authors upon request.

The $H_2$–$H_2$ potential anisotropy is relatively small; the values of $\sigma^2\bar{\Omega}_{2,2}$ calculated from $\bar{V}(r)$ are found to agree closely[14], e.g., to within about three significant figures at $T \geq 200$ K, with the corresponding result obtained from the complete potential energy surface of Ref. 15. The values obtained from the $dd'$ configuration are expected to yield better agreement[19];

**Table 3 H–H mean collision integrals (Å²)**

| $T$, K | $\sigma^2\bar{\Omega}_{1,1}$ | $\sigma^2\bar{\Omega}_{1,2}$ | $\sigma^2\bar{\Omega}_{1,3}$ | $\sigma^2\bar{\Omega}_{1,4}$ | $\sigma^2\bar{\Omega}_{1,5}$ | $\sigma^2\bar{\Omega}_{2,2}$ | $\sigma^2\bar{\Omega}_{2,3}$ | $\sigma^2\bar{\Omega}_{2,4}$ | $\sigma^2\bar{\Omega}_{3,3}$ |
|---|---|---|---|---|---|---|---|---|---|
| 100 | 9.732 | 9.091 | 8.681 | 8.383 | 8.139 | 10.760 | 10.200 | 9.795 | 9.910 |
| 150 | 9.013 | 8.469 | 8.093 | 7.810 | 7.582 | 9.902 | 9.390 | 9.007 | 9.223 |
| 200 | 8.561 | 8.047 | 7.691 | 7.413 | 7.182 | 9.326 | 8.844 | 8.465 | 8.760 |
| 300 | 7.955 | 7.470 | 7.114 | 6.824 | 6.561 | 8.554 | 8.082 | 7.710 | 8.101 |
| 400 | 7.536 | 7.049 | 6.676 | 6.373 | 6.113 | 8.015 | 7.560 | 7.198 | 7.616 |
| 500 | 7.207 | 6.713 | 6.338 | 6.053 | 5.769 | 7.608 | 7.195 | 6.841 | 7.234 |
| 600 | 6.948 | 6.435 | 6.060 | 5.728 | 5.447 | 7.286 | 6.849 | 6.507 | 6.923 |
| 700 | 6.716 | 6.206 | 5.783 | 5.439 | 5.208 | 7.031 | 6.584 | 6.219 | 6.633 |
| 800 | 6.505 | 5.977 | 5.557 | 5.248 | 4.991 | 6.793 | 6.342 | 6.002 | 6.392 |
| 900 | 6.318 | 5.768 | 5.375 | 5.063 | 4.799 | 6.585 | 6.136 | 5.811 | 6.200 |
| 1,000 | 6.136 | 5.603 | 5.210 | 4.895 | 4.622 | 6.384 | 5.964 | 5.642 | 6.026 |
| 1,500 | 5.488 | 4.959 | 4.559 | 4.242 | 3.982 | 5.703 | 5.284 | 4.950 | 5.338 |
| 2,000 | 5.032 | 4.505 | 4.118 | 3.822 | 3.585 | 5.226 | 4.820 | 4.516 | 4.868 |
| 3,000 | 4.403 | 3.892 | 3.522 | 3.213 | 2.925 | 4.607 | 4.244 | 3.984 | 4.218 |
| 4,000 | 3.962 | 3.447 | 3.041 | 2.704 | 2.409 | 4.204 | 3.882 | 3.639 | 3.731 |
| 5,000 | 3.609 | 3.075 | 2.655 | 2.300 | 2.003 | 3.923 | 3.615 | 3.369 | 3.354 |
| 6,000 | 3.311 | 2.767 | 2.329 | 1.972 | 1.679 | 3.702 | 3.402 | 3.087 | 3.051 |
| 8,000 | 2.831 | 2.262 | 1.831 | 1.502 | 1.263 | 3.301 | 2.910 | 2.579 | 2.549 |
| 10,000 | 2.451 | 1.896 | 1.480 | 1.207 | 1.002 | 2.937 | 2.534 | 2.193 | 2.196 |
| 12,000 | 2.148 | 1.611 | 1.248 | 0.999 | 0.823 | 2.616 | 2.224 | 1.886 | 1.924 |
| 14,000 | 1.906 | 1.393 | 1.068 | 0.847 | 0.694 | 2.382 | 1.967 | 1.642 | 1.705 |
| 16,000 | 1.708 | 1.229 | 0.928 | 0.730 | 0.597 | 2.162 | 1.755 | 1.440 | 1.526 |
| 18,000 | 1.544 | 1.093 | 0.819 | 0.642 | 0.523 | 1.973 | 1.579 | 1.288 | 1.377 |
| 20,000 | 1.406 | 0.982 | 0.727 | 0.571 | 0.464 | 1.810 | 1.428 | 1.158 | 1.250 |
| 22,000 | 1.288 | 0.890 | 0.657 | 0.512 | 0.415 | 1.668 | 1.304 | 1.049 | 1.145 |
| 24,000 | 1.187 | 0.812 | 0.597 | 0.464 | 0.376 | 1.544 | 1.197 | 0.958 | 1.053 |
| 26,000 | 1.100 | 0.746 | 0.546 | 0.423 | 0.342 | 1.436 | 1.104 | 0.880 | 0.975 |
| 28,000 | 1.023 | 0.688 | 0.502 | 0.388 | 0.315 | 1.339 | 1.023 | 0.811 | 0.905 |
| 30,000 | 0.956 | 0.638 | 0.464 | 0.359 | 0.289 | 1.254 | 0.953 | 0.755 | 0.845 |
| 32,000 | 0.896 | 0.595 | 0.431 | 0.333 | 0.268 | 1.178 | 0.890 | 0.704 | 0.791 |
| 35,000 | 0.818 | 0.539 | 0.389 | 0.300 | 0.240 | 1.078 | 0.810 | 0.639 | 0.721 |
| 40,000 | 0.712 | 0.465 | 0.333 | 0.256 | 0.205 | 0.945 | 0.700 | 0.548 | 0.626 |
| 50,000 | 0.562 | 0.359 | 0.256 | 0.194 | 0.160 | 0.747 | 0.552 | 0.422 | 0.496 |

**Table 4 $H_2$–$H_2$ mean collision integrals (Å²)**

| $T$, K | $\sigma^2\bar{\Omega}_{1,1}$ | $\sigma^2\bar{\Omega}_{1,2}$ | $\sigma^2\bar{\Omega}_{1,3}$ | $\sigma^2\bar{\Omega}_{1,4}$ | $\sigma^2\bar{\Omega}_{1,5}$ | $\sigma^2\bar{\Omega}_{2,2}$ | $\sigma^2\bar{\Omega}_{2,3}$ | $\sigma^2\bar{\Omega}_{2,4}$ | $\sigma^2\bar{\Omega}_{3,3}$ |
|---|---|---|---|---|---|---|---|---|---|
| 100 | 8.151 | 7.444 | 7.034 | 6.743 | 6.507 | 9.118 | 8.601 | 8.259 | 8.022 |
| 150 | 7.376 | 6.820 | 6.452 | 6.171 | 5.938 | 8.364 | 7.938 | 7.625 | 7.373 |
| 200 | 6.922 | 6.408 | 6.058 | 5.793 | 5.579 | 7.896 | 7.506 | 7.216 | 6.950 |
| 300 | 6.323 | 5.866 | 5.532 | 5.272 | 5.069 | 7.302 | 6.944 | 6.657 | 6.397 |
| 400 | 5.931 | 5.482 | 5.173 | 4.945 | 4.756 | 6.882 | 6.547 | 6.304 | 6.020 |
| 500 | 5.636 | 5.218 | 4.927 | 4.697 | 4.507 | 6.591 | 6.271 | 6.040 | 5.767 |
| 600 | 5.411 | 4.995 | 4.708 | 4.450 | 4.240 | 6.356 | 6.043 | 5.773 | 5.534 |
| 700 | 5.218 | 4.810 | 4.504 | 4.259 | 4.080 | 6.155 | 5.818 | 5.556 | 5.318 |
| 800 | 5.060 | 4.645 | 4.307 | 4.118 | 3.951 | 5.973 | 5.598 | 5.401 | 5.102 |
| 900 | 4.908 | 4.505 | 4.213 | 3.989 | 3.806 | 5.822 | 5.504 | 5.261 | 5.014 |
| 1,000 | 4.782 | 4.383 | 4.096 | 3.872 | 3.680 | 5.689 | 5.376 | 5.132 | 4.891 |
| 1,200 | 4.566 | 4.175 | 3.891 | 3.664 | 3.472 | 5.462 | 5.151 | 4.901 | 4.675 |
| 1,500 | 4.300 | 3.923 | 3.638 | 3.412 | 3.227 | 5.184 | 4.869 | 4.616 | 4.407 |
| 2,000 | 3.977 | 3.597 | 3.318 | 3.101 | 2.925 | 4.822 | 4.508 | 4.261 | 4.066 |
| 3,000 | 3.522 | 3.156 | 2.890 | 2.682 | 2.510 | 4.322 | 4.015 | 3.771 | 3.604 |
| 4,000 | 3.211 | 2.849 | 2.595 | 2.406 | 2.252 | 3.963 | 3.666 | 3.443 | 3.279 |
| 5,000 | 2.971 | 2.627 | 2.388 | 2.197 | 2.044 | 3.707 | 3.424 | 3.201 | 3.055 |
| 6,000 | 2.786 | 2.453 | 2.226 | 2.028 | 1.860 | 3.493 | 3.207 | 2.977 | 2.856 |
| 8,000 | 2.503 | 2.181 | 1.950 | 1.776 | 1.642 | 3.177 | 2.876 | 2.659 | 2.554 |
| 10,000 | 2.290 | 1.980 | 1.762 | 1.600 | 1.468 | 2.912 | 2.640 | 2.431 | 2.339 |

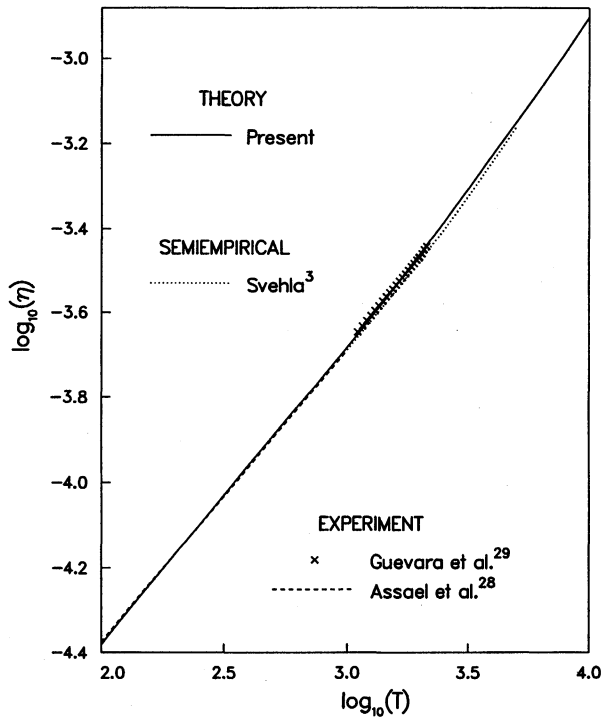


**Fig. 1 Viscosity for the interaction of $H_2$ molecules as a function of temperature. The calculations for determining the theoretical curve (solid line) are described in the text. The experimental curve (dashed line) at low $T$ is the fit of Ref. 28 to selected measured data. The data points at high $T$ are obtained from the relative measurements of Ref. 29 normalized to the value of the present calculation at 1615 K. The dotted line represents the semiempirical result of Ref. 3.**

in this case, we find agreement to within four significant figures. The values of the cross sections for high $E$ of the present work have been calculated directly from the average potential described earlier; the collision integrals for $H_2$–$H_2$ interactions are presented in Table 4. The expected accuracy (to within about 1%) of the results does not merit the number of significant figures shown in Tables 2 and 4; we have retained at least four significant figures, however, to facilitate interpolation of the data.

The result for the viscosity to second-order is compared with the correlation obtained by Assael et al.[28] from the measured low-$T$ data and with the measured values of Guevara et al.[29] at high $T$ in Fig. 1. We also show the semiempirical values of Ref. 3 at high $T$ that were determined by adjusting results obtained from valence-bond energies[30] to agree with a fit to the correlation of Ref. 28.

In addition, we have approximated the effects of vibrational excitation, occuring at the higher temperatures, with a Boltzmann average[31,32] of the cross sections obtained from the values of $\bar{V}(r)$ for the lowest vibrational states.[20] The result for the viscosity is only slightly lower than that shown in Fig. 1.

## Transport Properties

The application of $\sigma^2\bar{\Omega}$ is illustrated by an examination of the transport properties of a mixture of a gas composed of hydrogen atoms and molecules when excitation and ionization are not taken into account. For convenience, we present our results using reduced transport coefficients. The binary (self for a pure gas) diffusion coefficient $D$ in units of $cm^2/s$ can be obtained from a reduced coefficient $D^*$ defined by

$$pD^*(T) = 10^4 T^{-3/2} pD(T) = 26.287(2\mu)^{-1/2}/\sigma^2\bar{\Omega}_{1,1}(T) \quad (6)$$

similarly, the viscosity coefficient $\eta$ in units of gm/(cm s) is obtained from

$$\eta^*(T) = 10^6 T^{-1/2}\eta(T) = 26.696(2\mu)^{1/2}/\sigma^2\bar{\Omega}_{2,2}(T) \quad (7)$$

where $\sigma^2\bar{\Omega}$ is in $Å^2 = 10^{-16}$ $cm^2$. The physical constants required[22] for determining the coefficients of Eqs. (6) and (7) above were taken from Cohen and Taylor.[33]

The quantities $pD^*$ and $\eta^*$ are shown in Figs. 2 and 3, respectively, as a function of temperature. Note that $D^*$ for H–$H_2$ collisions does not lie between the H–H and $H_2$–$H_2$ curves as might be expected; this agrees with the behavior found in Ref. 2. Our results for the cross sections also support the explanation[2] for this abnormality; i.e., $Q_n^X$ is large because of the strong interaction energies of the ground state.

The curves for $\eta^*$ are shown in Fig. 4 for various values of the composition of a mixture gas. At low $T$, the quantity $\eta^*$ increases monatomically from its value for a pure H gas with increasing mole fractions $X(H_2)$ of hydrogen molecules; at high $T$, however, it reaches a maximum for $X(H_2)$ slightly larger than 0.5 and then falls with increasing $X(H_2)$ to its value for a pure $H_2$ gas.

We have calculated the thermal diffusion factor $\alpha$ to include the second (lowest) and third-order effects[22,34]; Fig. 5 shows $\alpha$ as a function of temperature for the various compositions of Fig. 4. Note that a temperature inversion[35] occurs for $T$ slightly below 3000 K; from low-order expressions,[22] one finds roughly that this temperature $T_i$ corresponds to

$$C^*(T_i) - 5/6 = 0 \quad (8)$$

where the reduced collision integral $C^*$ is defined[22] as the ratio $\sigma^2\bar{\Omega}_{1,2}/\sigma^2\bar{\Omega}_{1,1}$. The quantity $C^*$ can also be expressed[35] in terms of the derivative of $\sigma^2\bar{\Omega}_{1,2}$ with respect to $\ell n\ T$; combining this result with Eqs. (6) and (7) yields

$$(d/d\ \ell n\ T)\ell n(pD^*) = \tfrac{1}{2} \quad (9)$$

at $T_i$. Hence, the slope of $pD^*$ for the H–$H_2$ interaction reveals the existence of a $T_i$; note that the curvature of $pD^*$ shown in

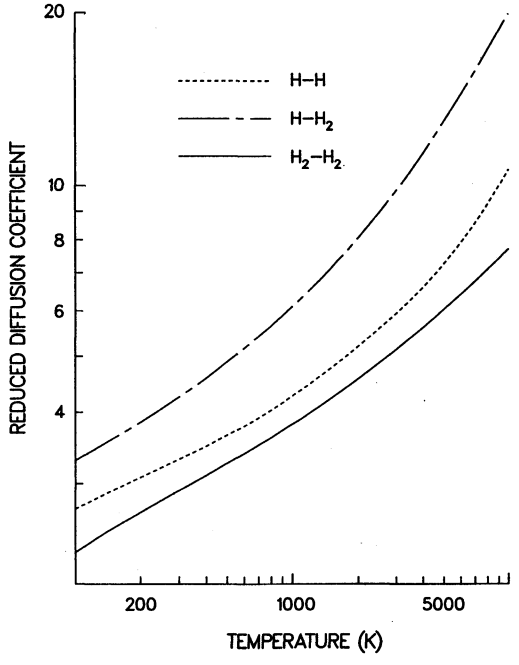


**Fig. 2 Quantity $pD^*$ calculated to third-order at a pressure of 1 atm as a function of temperature. The binary results for H–$H_2$ include a small correction for a 50/50 mixture (consisting of equal parts of atoms and molecules).**

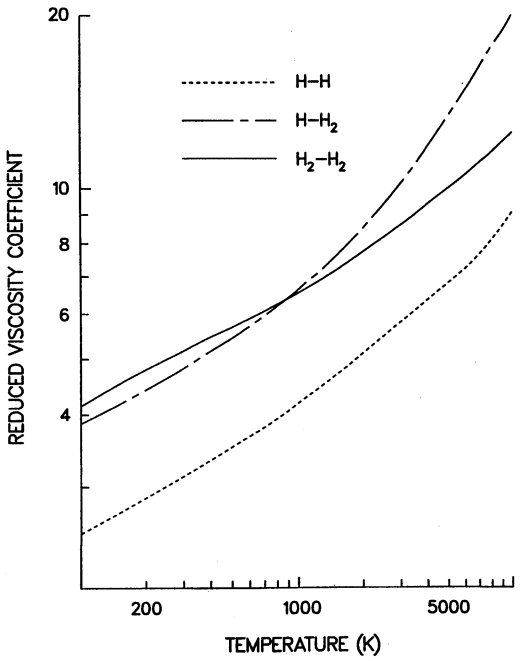


**Fig. 3 Quantity $\eta^*$ calculated to second-order as a function of temperature for various interactions.**

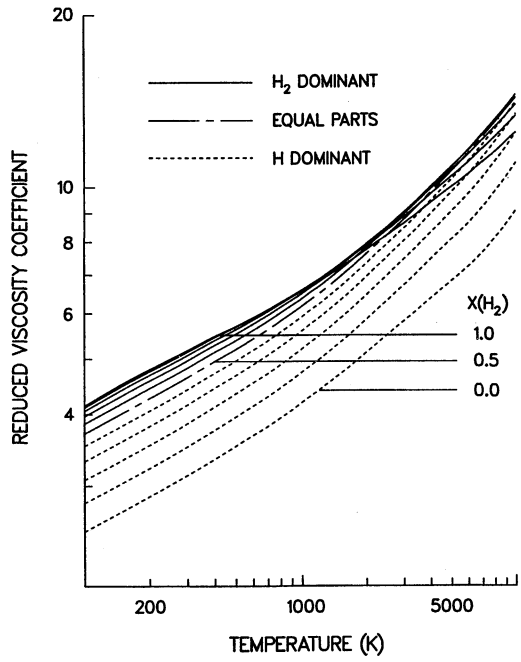


**Fig. 4 Quantity $\eta^*$ calculated to first-order as a function of temperature for various compositions of a hydrogen gas. The curves cover the range of the $X(H_2)$ from 0 to 1 in increments of 0.1. The dashed lines are determined for $X(H_2) < 0.5$, i.e., the H atoms provide the dominant composition of the gas, the long and short dashed curve represent $X(H_2) = 0.5$, and the solid lines are for $X(H_2) > 0.5$.**

Fig. 2 indicates that $pD^*$ is relatively sensitive to $T_i$. Using the values of Ref. 14 and Eq. (8), we find that $T_i$ is about 2800 K; from the calculated values of $\alpha$ for Fig. 4, we find more precisely that it is 2840 K, for example, for a mixture of equal parts of H and $H_2$. These results are about a factor 3 lower than the results of earlier work.[2] According to our formulation, it follows that $H_2$ and H migrate to the cooler and warmer regions, respectively, if $T$ is below $T_i$, and vice versa if $T$ is above $T_i$.[35] Note from Fig. 5 that the quantity $\alpha$ rises and falls

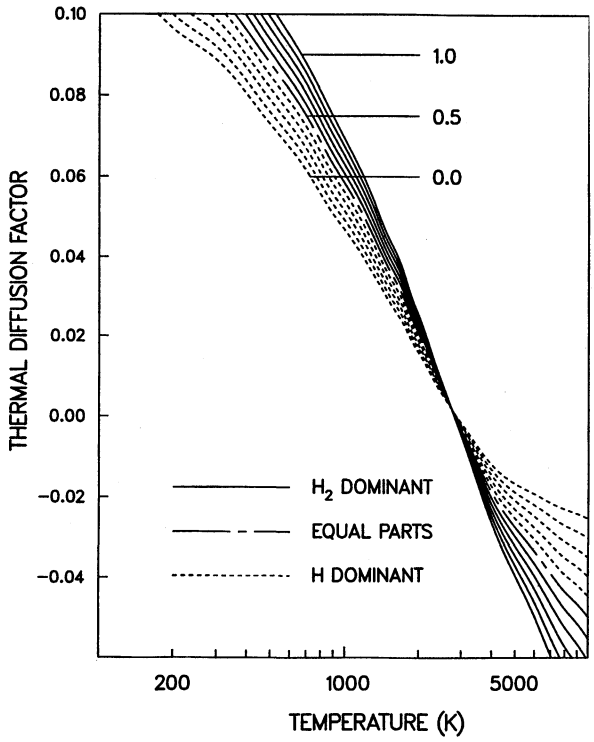


**Fig. 5 Quantity $\alpha$ calculated to third-order as a function of temperature for various compositions of a hydrogen gas. The composition of the curves is the same as that described in Fig. 4.**

monotonically with increasing $X(H_2)$ when $T$ is below and above $T_i$, respectively.

## Concluding Remarks

We have tabulated transport cross sections and collision integrals that are calculated from accurate potential energy data using approximations that have been tested by comparison with exact or measured results. The tabulated data have been applied to study the variation of the transport properties of a hydrogen gas with temperature and composition. In particular, the present results yield a significant improvement for thermal diffusion. In conclusion, we point out that our potential energy surfaces allow one to calculate the scattering for the vibrational transitions that are required for the determination of thermal conductivity.

## Acknowledgment

Support to Eugene Levin was provided by Contract NAS2-14031 from NASA to the Eloret Corporation is gratefully acknowledged.

## References

[1]Megli, T. W., Krier, H., and Burton, R. L., "Plasmadynamics Model for Nonequilibrium Process in $N_2/H_2$ Arcjets," *Journal of Thermophysics and Heat Transfer*, Vol. 10, No. 4, 1996, pp. 554–562.

[2]Vanderslice, J. T., Weissman, S., Mason, E. A., and Fallon, R.J., "High-Temperature Transport Properties of Dissociating Hydrogen," *Physics of Fluids*, Vol. 5, No. 2, 1962, pp. 155–164.

[3]Svehla, R. A., "Transport Coefficients for the NASA Lewis Chemical Equilibrium Program," NASA TM 4547, April 1995.

[4]Stallcop, J. R., Partridge, H., and Levin, E., "Analytical Fits for the Determination of the Transport Properties of Air," *Journal of Physics and Heat Transfer*, Vol. 10, No. 4, 1996, pp. 697–699.

[5]Partridge, H., Stallcop, J. R., and Levin, E., "Potential Energies and Collision Integrals for the Interactions of Air Components. I. *Ab initio* Calculation of Potential Energies and Neutral Interactions," *Molecular Physics and Hypersonic Flows*, edited by M. Capitelli, Kluwer, Dordrecht, The Netherlands, 1996, pp. 323–338.

[6]Stallcop, J. R., Bauschlicher, C. W., Partridge, H., Langhoff, S. R., and Levin, E., "Theoretical Study of Hydrogen and Nitrogen Inter-

actions: N–H Transport Cross Sections and Collision Integrals," *Journal of Chemical Physics*, Vol. 97, No. 8, 1992, pp. 5578–5585.

[7]Kołos, W., and Wolniewicz, L., "Potential-Energy Curves for the $X^1\Sigma_g^+$, $b^3\Sigma_u^+$, and $C^1\Pi_u$ States of the Hydrogen Molecule," *Journal of Chemical Physics*, Vol. 43, No. 7, 1965, pp. 2429–2441.

[8]Kołos, W., and Wolniewicz, L., "Variational Calculation of the Long-Range Interaction Between Two Ground-State Hydrogen Atoms," *Chemical Physics Letters*, Vol. 24, No. 4, 1974, pp. 457–463.

[9]Stallcop, J. R., Partridge, H., and Levin, E., "Potential Energies and Collision Integrals for the Interactions of Air Components. II. Scattering Calculations and Interactions Involving Ions," *Molecular Physics and Hypersonic Flows*, edited by M. Capitelli, Kluwer, Dordrecht, The Netherlands, 1996, pp. 339–349.

[10]Thakkar, A. J., "Higher Dispersion Coefficients: Accurate Values for Hydrogen Atoms and Simple Estimates for Other Systems," *Journal of Chemical Physics*, Vol. 89, No. 4, 1988, pp. 2092–2098.

[11]Partridge, H., Bauschlicher, C. W., Stallcop, J. R., and Levin, E., "*Ab initio* Potential Energy Surface for $H–H_2$," *Journal of Chemical Physics*, Vol. 99, No. 8, 1993, pp. 5951–5960.

[12]Bishop, D. M., and Pipin, J., "Vibrational Effects for the Dispersion-Energy and Dispersion-Polarizability Coefficients for Interactions Between H, He, and $H_2$," *Journal of Chemical Physics*, Vol. 98, No. 1, 1993, pp. 522–534.

[13]Tang, K. T., and Toennies, J. P., "A Model for the Potential Energy Surface of $H–H_2$ in the Intermediate and Long-Range Region," *Chemical Physics Letters*, Vol. 151, No. 3, 1988, pp. 301–307.

[14]Stallcop, J. R., Partridge, H., and Levin, E., "$H–H_2$ Collision Integrals and Transport Coefficients," *Chemical Physics Letters*, Vol. 254, No. 1, 1996, pp. 25–31.

[15]Schaefer, J., and Köhler, W. E., "Low Temperature Second Virial Coefficients of Para-$H_2$ Gas Obtained from Quantum Mechanical Pair Correlation Functions," *Zeitschrift fur Physik D—Atoms, Molecules and Clusters*, Vol. 13, No. 2, 1989, pp. 217–229.

[16]Scheafer, J., and Monchick, L., "Line Shape Cross Sections of HD Immersed in He and $H_2$ Gas. I. Pressure Broadening Cross Sections," *Journal of Chemical Physics*, Vol. 87, No. 1, 1987, pp. 171–181.

[17]Schaefer, J., and McKellar, A. R. W., "Faint Features of the Rotational $S_0(0)$ and $S_0(1)$ Transitions of $H_2$," *Zeitschrift fur Physik D—Atoms Molecules and Clusters*, Vol. 15, No. 1, 1990, pp. 51–65.

[18]Schaefer, J., and McKellar, A. R. W., "Faint Features of the Rotational $S_0(0)$ and $S_0(1)$ Transitions of $H_2$," *Zeitschrift fur Physik D—Atoms Molecules and Clusters*, Vol. 17, No. 2, 1990, p. 231.

[19]Stallcop, J. R., and Partridge, H., "The $N_2–N_2$ Potential Energy Surface," *Chemical Physics Letters*, Vol. 181, No. 1, 1996, pp. 212–220.

[20]Meyer, W., Borysov, A., and Fommhold, L., "Absorption Spectra of $H_2–H_2$ Pairs in the Fundamental Band," *Physical Review A*, Vol. 40, No. 12, 1989, pp. 6931–6949.

[21]Dymond, J. H., and Smith, E. B., "The Virial Coefficients of Pure Gases and Mixtures," Oxford Univ. Press, Oxford, England, UK, 1980.

[22]Maitland, G. C., Rigby, M., Smith, E. B., and Wakeham, W. A., *Intermolecular Forces. Their Origin and Determination*, Oxford Univ. Press, Oxford, England, UK, 1981.

[23]Parker, G. A., and Pack, R. T., "Rotationally and Vibrationally Inelastic Scattering in the Rotational IOS Approximation. Ultrasimple Calculation of Total (Differential, Integral, and Transport) Cross Sections for Nonspherical Molecules," *Journal of Chemical Physics*, Vol. 68, No. 4, 1978, pp. 1585–1601.

[24]Stallcop, J. R., Partridge, H., Walch, S. P., and Levin, E., "$H–N_2$ Interaction Energies, Transport Cross Sections, and Collision Integrals," *Journal of Chemical Physics*, Vol. 97, No. 5, 1992, pp. 3431–3436.

[25]Levin, E., Partridge, H., and Stallcop, J. R., "Collision Integrals and High Temperature Transport Properties for N–N, O–O, and N–O," *Journal of Thermophysics and Heat Transfer*, Vol. 4, No. 4, 1990, pp. 469–477.

[26]Levin, E., Schwenke, D. W., Stallcop, J. R., and Partridge, H., "Comparison of Semiclassical and Quantum Mechanical Methods for the Determination of Transport Cross Sections," *Chemical Physics Letters*, Vol. 227, No. 1, 1994, pp. 669–675.

[27]Stallcop, J. R., Partridge, H., and Levin, E., "Resonance Charge Transfer, Transport Cross Sections, and Collision Integrals for $N^+(^3P)–N(^4S^0)$ and $O^+(^4S^0)–O(^3P)$ Interactions," *Journal of Chemical Physics*, Vol. 95, No. 4, pp. 6429–6439.

[28]Assael, M. J., Mixafendi, S., and Wakeham, W. A., "The Viscosity and Thermal Conductivity of Normal Hydrogen in the Limit of Zero Density," *Journal of Physical and Chemical Reference Data*, Vol. 14, No. 4, 1986, pp. 1315–1322.

[29]Guevara, F. A., McInteer, R. B., and Wageman, W. E., "High-Temperature Viscosity Ratios for Hydrogen, Helium, Argon, and Nitrogen," *Physics of Fluids*, Vol. 12, No. 12, 1969, pp. 2493–2505.

[30]Vanderslice, J. T., and Mason, E. A., "Interaction Energies for the $H–H_2$ and $H_2–H_2$ System," *Journal of Chemical Physics*, Vol. 33, No. 2, 1960, pp. 492–494.

[31]Stallcop, J. R., Partridge, H., and Levin, E., "*Ab Initio* Potential Energy Surfaces and Electron-Spin-Exchange Cross Sections for $H–O_2$ Interactions," *Physical Review A*, Vol. 53, No. 2, 1996, pp. 766–771.

[32]Monchick, L., and Schaefer, J., "Theoretical Studies of $H_2–H_2$ collisions. II. Scattering and Transport Cross Sections of Hydrogen at Low Energies: Tests of a New *Ab Initio* Vibrotor Potential," *Journal of Chemical Physics*, Vol. 73, No. 12, 1980, pp. 6153–6161.

[33]Cohen, E. R., and Taylor, B. N., "The 1986 CODATA Recommended Values of the Fundamental Physical Constants," *Journal of Physical and Chemical Reference Data*, Vol. 17, No. 4, 1988, pp. 1795–1803.

[34]Mason, E. A., "Transport Properties of Gases Obeying a Modified Buckingham (Exp-Six) Potential," *Journal of Chemical Physics*, Vol. 22, No. 2, 1954, pp. 160–186.

[35]Hirschfelder, J. O., Curtiss, C. F., and Bird, R. B., *Molecular Theory of Gases and Liquids*, Wiley-Interscience, New York, 1964.